Use of Functional Maps in Renal Scintigraphy to Detect Segmental Arterial Lesions

Thomas B. Stibolt, Jr., John D. Bacher, N. Reed Dunnick, Allan Lock, A. Eric Jones, and James J. Bailey

National Institutes of Health, Bethesda, Maryland

Renography using a gamma camera, a minicomputer, [^{123}I]orthoiodohippurate ([^{123}I]OIH), and a canine model was employed to evaluate computer-generated maps of regional renal function. Renograms were obtained before and after ligations of the right renal arterial branch in four dogs, with subsequent angiographic and histologic confirmation of the lesions. Postoperative time-activity curves were normal. Washout and persistence index in three of four right kidneys showed regional abnormality. Functional renal mapping may provide a clinical technique for evaluating human renal vascular hypertension.

J Nucl Med 23: 291–295, 1982

Before the advent of the gamma camera, computer analysis of radionuclide renography was limited to subtraction of blood background from renograms obtained with a hand-held scintillation probe (*1*). Later the renographic curves were corrected for artifacts resulting from redistribution of the injected radionuclide bolus in the blood and tissues (*2*). These methods were limited to the detection of gross abnormalities of one or the other kidney.

The gamma camera allowed sequential images of the kidneys to be produced throughout the study, thereby yielding considerably more spatial information (*3,4*). When the camera data were captured directly by computer, it was further possible to extract time-activity curves over small regions of each kidney, encouraging investigators to attempt separation of cortical, medullary, and pelvic regions (*5*). This had potential use in differentiating various forms of renal dysfunction, especially parenchymal versus obstructive types (*6*).

Ultimately, one could derive time-activity curves for each pixel (picture element) of a digitized study. But display of 250 or so time-activity curves is confusing at best. Thus came about the development of the functional map, an image in which each pixel contains the value of a parameter extracted from that pixel's time-activity curve and presumably reflects renal function at that small region (*7*).

These maps have the important feature of displaying both spatial and temporal information in a single image, so that a local region of renal dysfunction can be appreciated more readily (*8,9*). We studied a group of 63 abnormal renal scintiphotos and found that in one third of the cases the functional maps revealed increased details concerning the location and nature (washin versus washout) of the abnormality. In the remaining cases the abnormality was so obvious that no additional information was revealed, though the dynamic nature of these abnormalities was accurately characterized by the functional map (*10*).

Despite the low counting statistics of [^{131}I]OIH used in the earlier study, the results suggested that functional maps might be particularly useful in detecting and characterizing early, mild, and/or small lesions. The availability of [^{123}I]OIH, which improves the counting statistics about 25 times owing to the shorter half-life and other factors, has made this use of functional maps appear even more promising (*11*).

We therefore decided to test this idea by studying segmental arterial lesions in a canine model using [^{123}I]OIH and functional maps.

Received July 24, 1981; revision accepted Oct. 19, 1981.

For reprints contact: A. Eric Jones, MD, Dept. of Nuclear Medicine, Bldg. 10, Room 1B 38B, National Institutes of Health, Bethesda, MD 20205.

MATERIALS AND METHODS

The studies were done in four foxhounds, each weighing approximately 50 lbs. The surgical procedure was as follows. The animals were premedicated with atropine and tranquilizer; anesthesia was induced intravenously and maintained by automatic ventilation. The right kidney was exposed via an abdominal route beneath the descending portion of the duodenum. The renal hilus was revealed by reflection of the perirenal fat, and a ventral segmental branch of the renal artery was ligated with 2-0 silk. The kidney was observed briefly for changes in appearance before closure.

Radionuclide renographic studies were performed on the dogs before the surgery and also 5 wk postoperatively. Contrast arteriograms were also done on both kidneys about 5 wk postoperatively. About 9 mo postoperatively, the right kidney was removed and examined histologically.

The radionuclide renographic studies were collected on a large-field-of-view (37 tube) gamma camera with a low-energy, high-resolution, parallel-hole collimator. The response was peaked for the 159 keV gamma for each study. [^{123}I]sodium orthoiodohippurate* was air freighted to the National Institutes of Health, where it was assayed for [^{123}I]OIH and other activities. The usual dose for a study was 5 mCi; doses up to 20 mCi were tried in some studies but failed to provide any apparent improvement in quality. The dogs were anesthetized with intravenous pentobarbital and held supine over the gamma camera by means of sandbags. Anesthetic and radionuclide were administered through the cephalic vein.

The data were acquired for 20 min from the gamma camera by the minicomputer system in LIST mode. After the study the data were reorganized into sequential 10-sec frames consisting of 64 × 64 (4096) pixels. Each kidney occupied about 175–200 pixels within each frame.

Subsequently the minicomputer system generated whole-kidney renograms (time-activity curves) and functional maps using previously described methods (*10,12,13*). Figure 1 shows the general shape of a time-activity curve and the parameters that are extracted

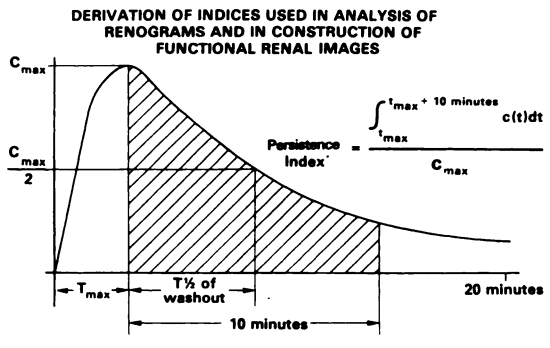

FIG. 1. Parameters (indices) used in functional mapping.

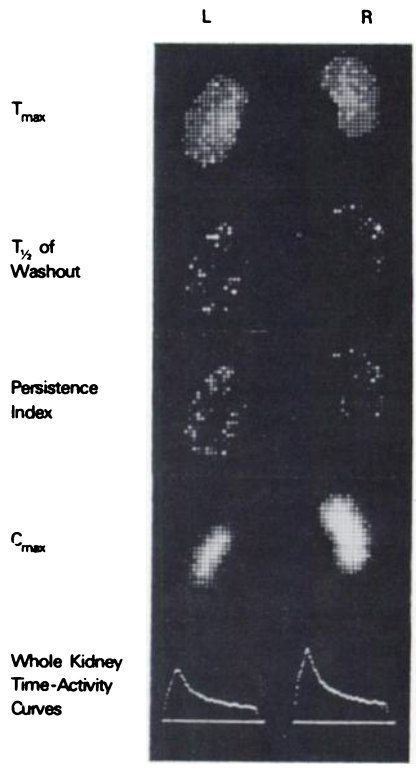

FIG. 2. Radionuclide study (dorsal view) before artery ligation.

pixel-by-pixel to form the functional maps. C_{max} indicates the maximum 10-sec count in the pixel at any time; T_{max} is the time at which that maximum occurred; $t_{1/2}$ is the time from the occurrence of the maximum until the counts decline to half that value. The persistence index (PI) is the area under the curve for a 10-min period starting at the maximum, normalized to the value of C_{max} for that pixel; the PI at a given pixel is equivalent to A/H (area/height) of ventilatory washout in pulmonary scintigraphic studies, which, as shown by Bunow et al. (*14*), approximates the theoretical time constant for washout of a single compartment.

RESULTS

All radionuclide studies before ligation and all postoperative studies of the nonligated left kidney were normal. All sequential renal images and all whole-kidney renograms were normal. Also, all radionuclide studies on Dog 4 were read as normal.

Figure 2 shows the normal renograms and functional maps from Dog 2 before ligation.

The T_{max} map shows some highlighting in the pelvic regions of both kidneys, indicating that the bulk of the radionuclide arrives there somewhat later than in the cortex, and is an entirely normal finding.

The $t_{1/2}$ and PI maps show a few, scattered highlighted pixels, most of which are isolated; in particular, there are no clusters of 20 or more adjacent $t_{1/2}$ pixels. Agress et al. (*10,12*) have shown this to be a frequent

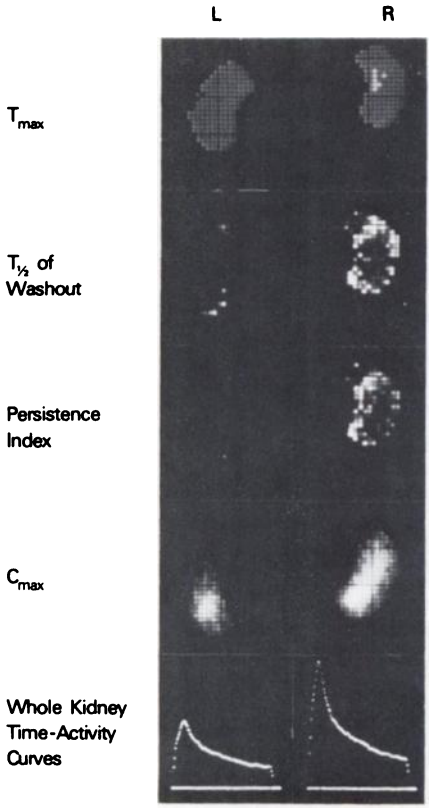

FIG. 3. Radionuclide study after ligation of segmental artery of right kidney (dorsal view). Note abnormality at edges.

finding in normal studies, relating to counting statistics and the signal-to-noise ratio of individual pixels.

The C_{max} appears brighter, and the peak amplitude of the renogram is higher, for the right kidney than for the left in this study, but the timing of the peak and the rapidity of washout are the same. It is difficult to maintain a foxhound's kidneys at a precisely level position because of the prominent spine. In this study the right kidney was closer to the gamma camera, thereby noticeably improving the counting efficiency; hence the brighter C_{max} map and higher renogram peak. In contrast, the T_{max}, $t_{1/2}$, and PI maps are not significantly affected by this level of difference.

Figure 3 shows the renograms and functional maps from Dog 2 after ligation of the segmental renal artery on the right. Note that there are large clusters of highlighted pixels in the $t_{1/2}$ and PI maps on the right. These same results were found in Dogs 1 and 3; the highlighted pixels tended to aggregate mainly in the upper pole. No such abnormalities appeared in the studies of Dog 4. The central mass of the kidney is not highlighted (see DISCUSSION below). Note also the very high peak in the right renogram and greater brightness of C_{max} there; as mentioned, this is related to the shorter distance between the right kidney and the detector, not to any abnormality of renal function.

Figure 4 shows the arterial phase of a contrast arteriogram of the right kidney of Dog 2. The arrow indicates the approximate location of the ligated (nonvisualized) segmental artery. Tortuous collateral arteries are faintly visible nearby. In contrast, the left renal arteriogram showed a regular branching of renal segmental arteries. The findings of contrast arteriogram on all four dogs were typified by this example.

Gross and microscopic examination of the right kidneys revealed well-demarcated areas of chronic diffuse atrophy and scarring in both the cortex and medulla (Fig. 5). The cortical mass was markedly decreased by tubular loss and atrophy. The atrophic glomeruli were surrounded by increased amounts of interstitial fibrous tissue (Fig. 5). Occasionally scant lymphocytic infiltrates were scattered in the interstitium. The medulla was also characterized by widespread tubular loss and increased fibrosis. In the absence of obvious infarction, these findings were considered compatible with chronic ischemia.

DISCUSSION

The functional map is an image that shows time-variant and spatial information is an easily assimilatable form. The alternative to this is for the reader to move between several images, attempting to compare regions against themselves and others—i.e., the usual method for reviewing scintigrams. Relatively subtle differences are easily missed under these conditions. There is no question that functional maps improve nuclear medicine diagnoses when added to the whole kidney's time-activity curves and the sequential images; that conclusion from our previous studies in humans (*10*) is confirmed by the present canine study. Moreover, this preliminary study indicates an increased usefulness of functional maps in

FIG. 4. Contrast arteriogram of right kidney. Arrow indicates location of ligated (nonvisualized) artery.

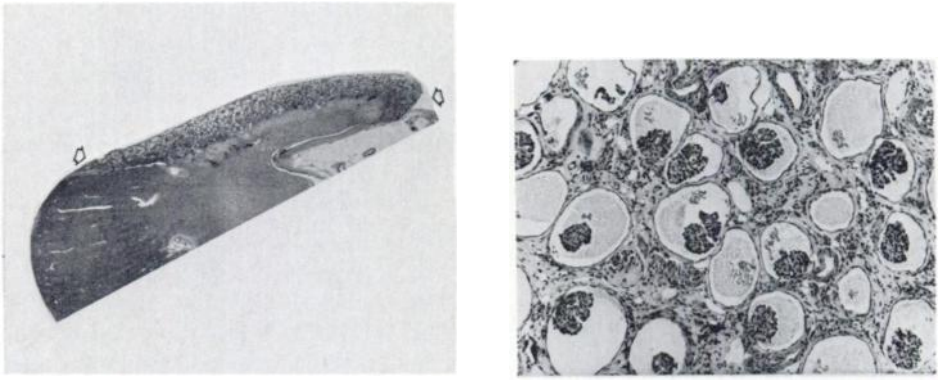

FIG. 5. Transverse upper-middle section of kidney, 9 mo after ligation of a ventral branch of right renal artery (left). Ventral area of chronic atrophy and progressive fibrosis is shown between arrows. Note mass of normal tissue dorsal to ventral lesion. High magnification of atrophic and fibrosed cortex (right). Most of the persistent glomeruli have shrunken tufts and dilated Bowman's spaces. Note severe tubular loss, interstitial fibrosis, and scanty lymphocytic infiltrates. (H&E × 100)

the detection and assessment of segmental renal-artery disease.

Interestingly, the abnormal area is revealed on the $t_{1/2}$ and PI maps but not on the C_{max} or T_{max} maps. We speculate that there is less glomerular filtrate in areas of decreased blood flow and hence less bulk flow to wash out the tubules; the resultant delay in washout would therefore produce abnormal values for the $t_{1/2}$ and PI parameters.

One would expect smaller values for C_{max} in the areas of decreased blood flow, but apparently they are not sufficiently smaller to show a definite abnormality on the C_{max} map. We don't completely understand this result. On the other hand, the absence of abnormalities on the T_{max} is quite understandable. The reason is that the transfer of orthoiodohippurate to the renal tissue is proportional to its concentration in the blood, and the blood is normally cleared of Hippuran by the remaining mass (both kidneys) of normally functioning renal tissue.

The preliminary study has also been useful in revealing certain technical problems. For example, since the gamma camera is dorsal to the kidney, it is possible that some of the ventral abnormality is masked out by a larger mass of normally functioning kidney lying dorsal to it (see Fig. 3). This could explain why no abnormality was seen in Dog 4 and why the abnormalities were most prominent at the edges of the kidney in the other dogs.

The delay in histologic examination of the kidneys occurred because originally its timeliness was not considered critical and therefore it received a low priority in scheduling. In retrospect, the size of the lesion suggests that the histologic examination should have been performed soon after the scintigraphic studies, or perhaps that the scintigraphic studies should have been repeated later, just before the histologic examination.

There are other technical problems. As noted in the normal study (Fig. 2), there can be scattered, isolated pixels with abnormal values because of poor counting statistics and a poor signal-to-noise ratio. This is more common in canine kidneys because of their smaller size compared with human kidneys. Also, the motion of the kidneys with respiration causes variations of a spatial nature that also degrade the signal-to-noise ratio. Such motion is minimized but not eliminated by studying the dogs in the supine position. This effect also tends to be minimized in lightly anesthetized dogs because the deep, slow (<10/min) pattern of respiration results in most of the data collection occurring in the resting position—i.e., with the lungs at functional residual capacity.

The results of this preliminary study have encouraged us to pursue a larger study: to measure the effects of these technical problems and to investigate methods for eliminating or minimizing them; to examine lesions of the dorsal and polar arteries as well as ventral segmental ones; to follow the lesions serially if possible; and to determine applicability to patients who are suspected of renal vascular hypertension.

FOOTNOTE

* Crocker Nuclear Laboratories.

ACKNOWLEDGMENTS

The authors thank Mr. Ray Farkas, Chief, Radiopharmacy for assuring the quality of radiopharmaceutical; Mr. Michael V. Green, Ms. Renée Dunham, and Dr. Steven Bacharach for assistance concerning collimation and data acquisition.

This work was presented in part at the 26th Annual Meeting of the Society of Nuclear Medicine (*J Nucl Med* 20: 659, 1979).

REFERENCES

1. BRITTON KE, BROWN NJG: The clinical use of (CABBS) renography: Investigation of the "nonfunctioning kidney" and renal artery stenosis by the use of ^{131}I-hippuran renography modified by computer assisted blood background subtraction (CABBS). *Br J Radiol* 41:570–579, 1968

2. SECKER-WALKER RH, SHEPHERD EP, CASSELL KJ: Clinical applications of computer-assisted renography. *J Nucl Med* 13:235-248, 1972
3. LOKEN MK, LINNEMAN RE, KUSH GS: Evaluation of renal function, using a scintillation camera and computer. *Radiology* 93:85-94, 1969
4. HALKO A, BURKE G, SORKIN A, et al: Computer-aided statistical analysis of the scintillation camera ^{131}I-hippuran renogram. *J Nucl Med* 14:253-264, 1973
5. WANG Y: Regional (compartmental) renogram for hypertension evaluation. *Am J Roent Rad Ther Nucl Med* 118: 842-851, 1973
6. FAIR WR: Renal perfusion/excretion determination renogram: A new tool in the diagnostic evaluation of renovascular hypertension. *J Urol* 113:595-600, 1975
7. WIENER SN, BORKAT FR, FLOYD RM: Functional imaging: A method of analysis and display using regional rate constants. *J Nucl Med* 15:65-68, 1974
8. ISHII Y, KAWAMURA J, MUKAI T, et al: Functional imaging of intrarenal blood flow using scintillation camera and computer. *J Nucl Med* 16:899-907, 1975
9. KAIHARA S, NATARAJAN TK, MAYNARD CD, et al: Construction of a functional image from spatially localized rate constants obtained from serial-camera and rectilinear scanner data. *Radiology* 93:1345-1348, 1969
10. AGRESS H JR, LEVENSON SM, GELFAND MJ, et al: Functional mapping and related computer-generated images in radionuclide renography. *Appl Radiol* 5:202-208, 1976
11. ZIELINSKI FW, ROBINSON GD JR, LEE AW, et al: ^{123}I-sodium O-iodohippurate for computer-assisted renography. *Trans Am Nucl Soc* 22:118, 1975
12. AGRESS H JR, LEVENSON SM, GELFAND MJ, et al: Application of computer-generated functional (parametric) maps in radionuclide renography. In *ORNL Proceedings of Fifth Symposium on Sharing of Computer Programs and Technology in Nuclear Medicine.* Publication #750124, Salt Lake City, USAEC, 1975, pp 180-194
13. GELFAND MJ, ALLEN FH, GREEN MV, et al: Functional mapping of renal transit of ^{131}I-iodohippuran. In *ORNL Proceedings of Third Symposium on Sharing of Computer Programs and Technology in Nuclear Medicine.* Publication #730627, Miami, USAEC, 1973, pp 100-112
14. BUNOW B, LINE BR, HORTON MR, et al: Regional ventilatory clearance by xenon scintigraphy: A critical evaluation of two estimation procedures. *J Nucl Med* 20:703-710, 1979